END-TO-END PIPELINE FOR FOURIER DOMAIN OPTICAL COHERENCE TOMOGRAPHY OF HUMAN OPTIC NERVE HEAD

Sieun Lee, Mei Young, Marinko V. Sarunic, Mirza Faisal Beg
School of Engineering Science, Simon Fraser University
Correspondence: Sieun.Lee@sfu.ca

INTRODUCTION

Glaucoma, the second leading cause of blindness world-wide, is progressive and irreversible loss of vision due to damage in optic nerve. Elevated intra-ocular pressure (IOP) has been identified as a major risk factor [3]; however the significant variance in individual IOP and glaucoma susceptibility has not been fully understood. Recent histological studies on non-human primates suggest biomechanical effects of IOP on the tissues of the Optic Nerve Head (ONH) - a central depression in posterior retina where the optic nerve fibre exits the eye toward the brain - play a central role in the development and progression of the disease [4]. These findings point to fundamental understanding of glaucoma pathology and susceptibility based on structural attributes, potentially leading to early detection and treatment which are crucial due to the irreversible nature of the disease. Further investigation among human patients necessitates a means to non-invasively monitor and computationally analyze in-vivo ONH structures.

In the past decade, optical coherence tomography (OCT) has emerged as a powerful and versatile imaging tool in biomedicine. The OCT system is relatively inexpensive and compact and the imaging procedure is simple, fast and non-invasive. The resulting images provide a high-resolution, three-dimensional, cross-sectional view of biological tissues in-vivo. In ophthalmology and vision science, recently commercialized products and novel prototypes have generated in-depth view of anterior and posterior ocular segments. Computational algorithms have been developed to automatically extract from the volumetric images clinically relevant information such as thickness of retinal layers [1] and area of optic disc [2]. Such morphometric analysis combined with traditional clinical images and functional tests enables sensitive monitoring of pathophysiology and quantitative measurement in longitudinal and cross-sectional studies, providing singular insights to clinicians and researchers.

In this paper, we present a comprehensive system of OCT imaging and morphometric analysis of human ONH developed as a collaborative effort of Biomedical Optics Research Group (BORG) and Medical Image Analysis Lab (MIAL) at Simon Fraser University, and an ophthalmologist at the Eye Care Centre at Vancouver General Hospital. An end-to-end pipeline overview of the system - from data acquisition of a subject's ONH to clinically valuable information – is given with an extended section on motion artifact correction. A graphical representation of the pipeline is shown in Figure 1.

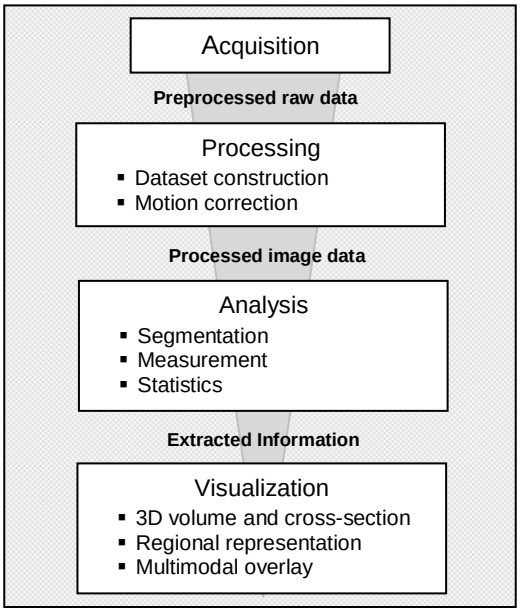

Figure 1**:** BORG-MIAL OCT Analysis Pipeline

OCT IMAGE ACQUISITION

FD-OCT is a relatively recent development from the original time-domain OCT. It uses a broadband light source and spectral data acquisition to dramatically reduce acquisition time and improve the signal to noise ratio. Broadband light from superluminescent diode is split into the reference arm and the sample arm. At the end of the sample arm, the beam travels past subject's anterior ocular segment and focuses in the ONH region, penetrating into neural and vascular cells while scattering at different structures and layers. This scattered beam is retuned and recombined with the reference beam, creating interference. The interferometric fringes contain

backscattering depth information from the sample, and this combined with two-dimensional scanning mirrors generates cross-sectional, three-dimensional intensity data, revealing structures within ONH.

The mirror scanning pattern is pre-programmed, typically in raster format. The subject is seated in front of a standard slit lamp on which the imaging optics is mounted. Acquisition duration is nominally 8 seconds and 2mm x 2mm x 1.7mm region centered at ONH is scanned in 1024 x 800 x 200 voxels. During acquisition, custom in-house developed software called *OCTViewer* controls scanning and data collection, and performs a series of real-time signal processing before displaying image in a movie format. The preprocessing steps include resampling of spectrometer data, dispersion compensation, and fast Fourier transform.

OCT IMAGE PROCESSING: MOTION CORRECTION

Preprocessed raw data in binary stream is first reconstructed into a volumetric image array. Contrast enhancement and noise filtering may be performed to improve image quality. The most severe artifact remaining is caused by subject motion relative to imaging setup. This will be discussed in detail along with methods of correction.

During the 8 seconds of image acquisition, the eye is in constant motion, of which the effect is magnified by the small physical dimension of the acquired image. Use of a chin rest, forehead support, and fixation target may reduce head and body movement to a certain degree. Nevertheless the eye remains in continual, involuntary *fixational eye movements*: tremor, drift, and microsaccades [5]. Tremor is wave-like motion with small amplitude and high frequency (~90Hz) in the range of system resolution and unlikely to be detected. Drift occurs gradually in a relatively low speed, and does not compromise the image quality significantly. Microsaccades are the largest fixational eye movements occurring in short twitches. The duration and frequency make microsaccades the most visible source of image corruption. OCT imaging with eye tracking has been implemented by few research groups and in the latest line of commercialized systems. This involves instant adjustment of acquisition beam path to compensate for the eye motion [6]. However eye tracking requires substantial and costly modification to the standard OCT setup which is not always feasible. Post-acquisition correction methods are thus needed.

Correcting a motion-affected image requires either i) image of whole or part of the subject without motion as the ground-truth data, or ii) information about the motion. In our present case clean data unaffected by subject motion is impossible to obtain unless by invasive means. There is also no anatomical feature in ONH to serve as a definite and reliable universal landmark as the topology varies considerably among subjects. Motion itself is a composite of different translational and rotational movements in three-dimension occurring concurrently, each varying between subjects and imaging sessions. Thus, the exact characterization of the motion needed to produce a rigorous and complete solution to the motion problem can be very complex. Fortunately, clinical knowledge and general trend observed in a large number of datasets allow us to make few reasonable assumptions. The next few paragraphs outline how these assumptions are made and how the problem is simplified and rectified in each step.

First we determine the unit of image subset that is 'unaffected' by motion in practical sense, based on scanning speed and known motion frequency and duration. The system line rate of 20,000 Hz allows acquisition of a single line in 50μs and a single frame consisting of 800 lines in 0.04s. This is at a much higher frequency than any movement with noticeable amplitude (including microsaccades which do not exceed 5Hz) [5], and we take a single frame as instantaneous, uncorrupted image called a B-scan. These motionless 2D cross-sections and existing clinical knowledge serve as an alternative to a full 3D ground-truth dataset. By symmetry, any other axial cross-section of a volume reconstructed from the motionless cross-sections are expected to have similar level of smoothness in feature boundaries and layers, and any sharp spike or pseudo-periodic oscillating pattern are assumed to be artifacts. ONH is treated as a rigid object that does not twist, morph, or scale; any movement at a point in time affects the subject as a whole.

With the motionless B-scan, the problem focuses on finding the motion between consecutive fast scans. The differences between the n^{th} and $n^{th} + 1$ frame are due to a combination of scanning beam position shift and subject motion. Distinguishing between these two is the key to restoring a volumetric retinal image without motion artifact. An analogy to this is, in a series of video frames, tracking a moving object that is also deforming at the same time. In raster scan OCT, the deformation is analogous to different view in each frame as the scanning beam moves across the imaging space, generating an ordered row of 200 frames (fast scans) in a single orientation. In this perspective, we are forced to exclude the motion in the direction normal to the frame plane, or 'in the line of the camera', because such motion causes skewing or scaling in the image that is difficult to distinguish from deformation. The motion between n^{th} and $n^{th} + 1$ frame is thus restricted to translation and rotation in the frame plane.

Maximum Cross-Correlation Correction

One of seminal early papers [7] on OCT proposed correcting motion artifact in 2D OCT images using maximum cross-correlation of adjacent columns. This simple and effective method is easily extended to three-dimensions. Each frame is translated in reference to the next frame, and at each displacement cross-correlation between the frames is computed. The displacement yielding maximum correlation is noted as the blue high-frequency curve in Figure 2a. The cross-correlation is measure of similarity between two frames, and reciprocally the displacement of maximum correlation represents the spatial difference. Because the frames are densely located in space and correlation is computed on entire frame in 2D, regional anatomical differences in adjacent frames due to scanning (ex. blood vessel protrusion) contributes far less than frame-wide shift due to subject motion (ex. entire ONH moving up). This is the central idea behind maximum cross-correlation correction.

A common practice is therefore displacing each frame by the amount of maximum correlation displacement. However this neglects the fact that the frame-to-frame global shift may occur not only by subject motion but also the natural curvature of the eye, which is lost in the process of flattening the maximum correlation profile. The rapid change in topology in the optic cup region is also likely to affect correlation between frames. Therefore the correction by simple flattening can be particularly problematic in ONH imaging. A more appropriate approach is fitting a smooth curve to the maximum correlation profile to preserve the curvature. Figure 2b is a reconstructed cross-section orthogonal to the fast scans such that each column is a line from a single fast scan. The effect of the subject motion is evident in the wave-like artifact. In Figure 2c the frames have been displaced to flatten the maximum correlation profile by fitting it to the straight line in Figure 2a. The frames in the center of the cup region are shifted more upward than the rest, and this ends up reducing the cup depth in the center. In Figure 2d the frames have been shifted to compensate only for the oscillatory artifact without changing the overall curve of the maximum correlation profile by fitting it to the smooth curve in Figure 2a. The fitting curve is chosen qualitatively based on the curvature in fast scans, since the eye is nominally spherical and axially symmetric.

There are several limitations to maximum cross-correlation correction. First, the rotational component of the motion is neglected, as it becomes computationally impractical to calculate correlation for all combinations of rotation and translation. Second, correlation in lateral direction (left-to-right) is less reliable than axial direction (up-and-down), because there are strong edges in the axial direction but often not in lateral direction, and except in the cup region where there are stiff vertical slopes, correlation does not accurately reflect lateral translation. This is similar to the 'windowing problem' in computer vision where ambiguity arises from the camera imaging only part of object boundary. Computing the correlation coefficient, which accounts for both correlation and anti-correlation, is more robust in this regard than simple cross-correlation but not adequately so. Although maximum cross-correlation correction is effectively applicable only in axial translation, it is still widely used because of its simplicity and surprising good result, as shown in Figure 3a and b.

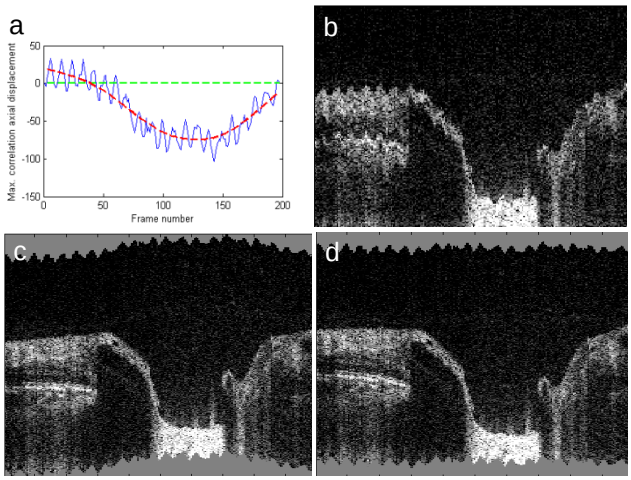

Figure 2 a. maximum correlation profile b. motion affected cross-section c. 'flattened' correction d. smooth-curve correction

Alternative Methods

One method of axial motion correction is using additional orthogonal scans for registration [8]. Each frame position is compensated by maximum-correlation-matching the intensity profile along lines of intersection with the registration scans. This method eliminates the need for curve fitting and possibly results in more accurate topology restoration. However the registration scans needs to be at precise locations relative to the frames, which may be difficult to achieve with acquisition time difference between the registration scans and other frames.

Scanning laser ophthalmoscopy (SLO) produces an artifact-free, traditional 2D en-face (in the direction a clinician looks into a patient's eye) view of the eye. A similar en-face view can be constructed from volumetric OCT data by summing voxels in axial direction. Matching blood vessels in these en-face images by image registration and warping the volume accordingly has been shown effective in correcting lateral motion [9], but this method does not address the axial motion.

OCT IMAGE ANALYSIS

The processed volumetric image is ready for extraction of information. Analysis steps are specific to research questions, and generally involve establishing an appropriate morphometric parameter, measuring it across multiple datasets, and identifying statistical trend in relation to disease pathology. Here we focus on comparison of optic cup depth and volume which were shown to increase with progression of glaucoma in monkey models [4].

Post-BMO optic cup is defined as the region bounded by inner limiting membrane (ILM) and the plane of Bruch's Membrane Opening (BMO). Trained raters manually segmented the ILM and BMO in each volume as shown in Figure 3c. Detailed protocol and Amira script was written and implemented to limit bias and inter- and intra-rater validation is performed.

From the segmentation in Figure 3c, smooth mesh surface is constructed from ILM points, and least-squares plane is fitted to BMO points. Measuring the distance between the ILM surface and BMO plane yields optic cup depth. The total number of voxels enclosed between ILM and BMO plane yields post-BMO optic cup volume. These are measured across the dataset and the result is evaluated for statistical inference.

ONH VISUALIZATION

Visualization, such as the colour-coded 3D optic cup depth map in Figure 3d, is an integral part of the pipeline. Graphical representations of intermediate and final result aid in decision-making. This is also a valuable tool for end-users - clinicians and vision scientists can examine the ONH structure in 3D volume and cross-sections in conjunction with traditional clinical images, and intuitively understand and interpret the computational results.

CONCLUSION

We have developed an end-to-end pipeline of 3D OCT image acquisition and analysis for human ONH. Subject motion causes significant artifact which can affect all downstream measurement and analysis in the pipeline. Axial motion correction by smoothing maximum cross-correlation profile has produced satisfactory results, and further investigation will focus on concurrent lateral and rotational motion correction. Motion-corrected volumetric data is analyzed to extract relevant information and draw statistical inference.

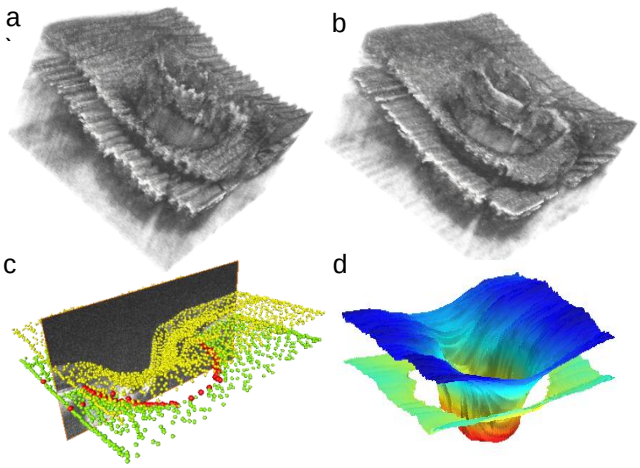

Figure 3 a. Data before and b. after axial motion correction c. segmentation of ILM and BM d. colourmap of optic cup depth in reference to BM plane

ACKNOWLEDGEMENTS

We acknowledge support from a NSERC/CIHR CHRP Grant, and MSFHR Career Investigator Award to MVS and MFB.

REFERENCES

[1] D.C. Fernandez, H.M. Salinas, and C.A. Puliafito, "Automated detection of retinal layer structures on optical coherence tomography" *Optics Express*, vol. 13, issue 25, pp. 10200-10216, 2005.

[2] K. Lee, M. Niemeijer, M.K. Garvin, Y.H. Kwon, M. Sonka and M.D. Abramoff, "Segmentation of the optic disc in 3-D OCT scans of the optic nerve head" *IEEE Transactions on Medical Imaging*, vol. 29, no. 1, pp. 159-168, January 2010.

[3] A. Heijl, M.C. Leske, B. Bengtsson, L. Hyman, B. Bengtsson, and M. Hussein, "Reduction of intraocular pressure and glaucoma progression," *Arch Ophthalmol*, vol. 120, no. 10, pp. 1268-1279, 2002.

[4] J.C. Downs, M.D. Roberts, and C.F. Burgoyne, "The mechanical environment of the optic nerve head in glaucoma" *Optom Vis Scie.*, vol. 85, no. 6, pp. 425-435, 2008

[5] S. Martinez-Conde, S.L. Macknick, and D.H. Hubel, "The role of fixational eye movements in visual perception," *Nature Neuroscience.*, vol. 5, pp. 229-240, 2004.

[6] M. Pircher, B. Baumann, E. Gotzinger, H. Sattmmann and C.K. Hitzenberger, "Simultaneous SLO/OCT imaging of the human retina with axial eye motion correction," *Opt Express, vol. 15 no. 25 pp.16922-32,2007.*

[7] M.R. Hee, J.A. Izatt, E.A. Swanson, D. Huang, J.S. Schuman, C. P. Lin, C.A. Puliafito, J.G. Fujimoto, "Optical coherence tomography of the human retina," *Arch Opthalmol.,* vol. 113, no. 3, pp.325-332, 1995.

[8] B. Potsaid, I. Gorczynska, V.J. Srinivasan, Y. Chen, J. Jiang, A. Cable, and J.G. Fujimoto, "Ultrahigh speed spectral / Fourier domain OCT ophthalmic imaging at 70,000 to 321,500 axial scans per second", *Opt Express*, vol.15, no. 19, pp. 15149-15169, 2008.

[9] S. Ricco, M. Chen, H. Ishikawa, G. Wollstein, and J. Schuman, "Correcting motion artifacts in retinal spectral domain optical coherence tomography via image registration," *MICCAI 2009,* part 1, LNCS 5761, pp. 100-107, 2009,